

Polaronic behavior of undoped high- T_c cuprates

O. Rösch¹, O. Gunnarsson¹, X. J. Zhou^{2,3}, T. Yoshida⁴,

T. Sasagawa⁵, A. Fujimori⁴, Z. Hussain³, Z.-X. Shen² and S. Uchida⁴

¹Max-Planck-Institut für Festkörperforschung, D-70506 Stuttgart, Germany

²Department of Applied Physics and Stanford Synchrotron Radiation Laboratory, Stanford University, Stanford, California 94305, USA

³Advanced Light Source, Lawrence Berkeley National Lab, Berkeley, California 94720, USA

⁴Department of Physics and Department of Complexity Science and Engineering, University of Tokyo, Tokyo, 113-0033, Japan

⁵Department of Advanced Materials Science, University of Tokyo, Japan

We present angle-resolved photoemission spectroscopy (ARPES) data on undoped La_2CuO_4 , indicating polaronic coupling between bosons and charge carriers. Using a shell model, we calculate the electron-phonon coupling and find that it is strong enough to give polarons. We develop an efficient method for calculating ARPES spectra in undoped systems. Using the calculated couplings, we find the width of the phonon side band in good agreement with experiment. We analyze reasons for the observed dependence of the width on the binding energy.

An important issue in the discussion of high- T_c cuprates is the relative importance of couplings to phonons and spin fluctuations. Recent angle-resolved photoemission spectroscopy (ARPES) work for undoped or weakly doped $\text{Ca}_{2-x}\text{Na}_x\text{CuO}_2\text{Cl}_2$ shows polaronic behavior [1]. A broad \mathbf{k} -dependent boson side band was observed, while a quasi-particle, if present, was too weak to be seen. This raises important questions about the nature of the bosons coupling to the electrons. Here we present experimental data for $\text{La}_{2-x}\text{Sr}_x\text{CuO}_4$, showing similar boson side bands. Using a shell model, we calculate the electron-phonon coupling for undoped La_2CuO_4 . We find that the coupling is sufficiently strong to give polaronic behavior. We develop a method for calculating spectra of a t - J model with many phonon modes and at finite temperature. The calculated couplings give side band widths in good agreement with experiment. The dependence of the width on the binding energy is analyzed. This work shows that the electron-phonon coupling plays an important role for properties of undoped cuprates.

The photoemission measurements were carried out on beamline 10.0.1 at the Advanced Light Source. The photon energy was 55 eV and the energy resolution was ≈ 18 meV. The La_2CuO_4 single crystals were grown by the traveling solvent floating zone method. The samples were cleaved *in situ* in vacuum with a base pressure better than 4×10^{-11} Torr and measured at a temperature of ≈ 20 K. The data are shown in Fig. 1. There are broad boson side bands at about 0.5 eV binding energy, similar to the results for $\text{Ca}_{2-x}\text{Na}_x\text{CuO}_2\text{Cl}_2$ [1].

To see if these boson side bands can be explained by the coupling to phonons, we calculate the electron-phonon interaction. We use a shell model [2] that successfully describes phonon dispersions in several cuprates to obtain the phonon modes in La_2CuO_4 . Within this model the change in the electrostatic potential induced by each mode is calculated to first order in the atomic displacements. This gives rise to a linear coupling between doped charges and the phonons. We use the t - J

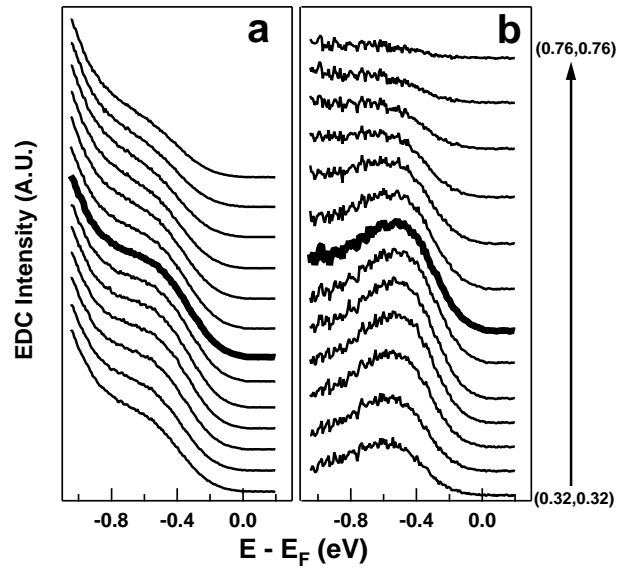


FIG. 1: (a) Photoemission spectra of La_2CuO_4 along the $(0,0)$ - (π,π) nodal direction in the first Brillouin zone. The corresponding momentum runs from $(0.32, 0.32)\pi$ to $(0.76, 0.76)\pi$, as indicated by the arrow. (b) To highlight the momentum dependence, a "background" given by a spectrum near (π,π) was subtracted from the spectra. The bold curves correspond to a momentum near $(\pi/2, \pi/2)$.

model to describe the electronic degrees of freedom in the CuO_2 planes. Doped holes form Zhang-Rice singlets with the spins of Cu d holes with their additional charge distributed symmetrically on the four neighboring O p orbitals. This charge distribution couples to the modulation of the electrostatic potential caused by the phonons. Since the undoped system is an insulator, screening in the shell model is only provided by the displacement of the shells against the atomic cores. In addition, there is coupling from the modulation of the p - d hopping t_{pd} and the charge-transfer energy in the three-band model from which the t - J model is derived [3]. We include the

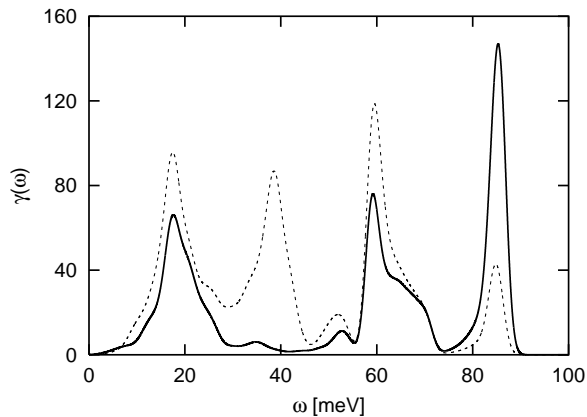


FIG. 2: Spectral distribution of coupling to singlets (full line) and to holes in non-bonding O p orbitals (dashed line). A Gaussian broadening (FWHM=3 meV) was used.

dominant on-site terms. The modulation of the charge-transfer energy is calculated from the modulation of p and d level energies within the shell model instead of assuming a nearest-neighbor Coulomb repulsion U_{pd} as in Ref. [3]. The shell model calculations are done on a $(30)^3$ mesh in \mathbf{q} space using the high-temperature tetragonal structure from Ref. [2] but similar results are obtained for the low-temperature orthorhombic structure. The results depend on the eigenvectors of the shell model. Since the shell model [2] describes neutron scattering intensities well, the eigenvectors are believed to be accurate [4].

The electron-phonon interaction is then given by

$$H_{ep} = \frac{1}{\sqrt{N}} \sum_{\mathbf{q}\nu} g_{\mathbf{q}\nu} (1 - n_i) \sqrt{2\omega_{\mathbf{q}\nu}} Q_{\mathbf{q}\nu} e^{i\mathbf{q}\cdot\mathbf{R}_i}. \quad (1)$$

This is an on-site coupling to empty sites representing singlets in the t - J model. It is linear in the generalized phonon coordinates $Q_{\mathbf{q}\nu}$ and the strength is given by the coupling constants $g_{\mathbf{q}\nu}$. A phonon mode with eigenfrequency $\omega_{\mathbf{q}\nu}$ is labeled by its wave vector \mathbf{q} and branch index ν . n_i measures the occupancy at site \mathbf{R}_i . The number of sites is N .

Introducing the dimensionless coupling constant $\lambda \equiv 2 \sum_{\mathbf{q}\nu} |g_{\mathbf{q}\nu}|^2 / (8t\omega_{\mathbf{q}\nu}N)$, we obtain $\lambda = 1.2$ [6] for $t = 0.4$ eV. The criterion for polaronic behavior in the Holstein- t - J model is $\lambda > \lambda_c = 0.4$ [5]. If the next-nearest neighbor hopping integral t' is taken into account, λ_c should increase. The coupling derived for undoped La_2CuO_4 should, nevertheless, be strong enough to cause polaronic behavior, as observed experimentally.

Fig. 2 shows the spectral distribution $\gamma(\omega) \equiv \sum_{\mathbf{q}\nu} |g_{\mathbf{q}\nu}|^2 / (\omega_{\mathbf{q}\nu}N) \delta(\omega - \omega_{\mathbf{q}\nu})$ of our coupling (full line). A peak around 20 meV can be attributed mainly to modes involving La whereas the spectral weight at 60-70 meV is mainly due to vibrations of the apical O. A peak around 85 meV is caused by the planar O (half-)breathing mode coupling predominantly via the

t_{pd} modulation. This energy dependence of the coupling agrees qualitatively with the observation of fine structures in the electron self-energy of $\text{La}_{2-x}\text{Sr}_x\text{CuO}_4$ [7], except that the calculation does not give appreciable coupling around 40 meV. This could be due to surface effects or distortions due to doping [8, 9, 10]. Such effects would be missing in our calculation, which is performed for an ideal La_2CuO_4 structure. For comparison, the dashed line in Fig. 2 shows the spectral distribution of the coupling to holes in individual non-bonding O p orbitals.

To discuss the \mathbf{q} dependence of the coupling we sum $|g_{\mathbf{q}\nu}|^2$ over all modes and the phonon momentum q_z perpendicular to the CuO_2 planes. The coupling increases with decreasing $|(q_x, q_y)|$ although some individual modes show different behavior, e.g. the coupling to the O (half-)breathing mode peaks around (π, π) .

Based on Ref. [11] we have developed an efficient method for calculating ARPES spectra in undoped systems at a finite temperature T . Using an adiabatic approximation, the spectral function for creating a hole with momentum \mathbf{k} in an undoped system is written as

$$A_{\mathbf{k}}(\omega, T) = \int d\mathbf{Q} |\phi_0(\mathbf{Q}, T)|^2 \rho_{\mathbf{k}}(\mathbf{Q}, \omega). \quad (2)$$

The integration is over all phonon coordinates $Q_{\mathbf{q}\nu}$ summarized in the vector \mathbf{Q} . $\rho_{\mathbf{k}}(\mathbf{Q}, \omega)$ is the spectrum calculated for the electronic system in a distorted lattice (characterized by \mathbf{Q}). No dynamic phonons are included in the calculation of $\rho_{\mathbf{k}}(\mathbf{Q}, \omega)$, since the distortions \mathbf{Q} are treated as c -numbers and only give rise to static on-site energies in the Hamiltonian (1).

$$|\phi_0(\mathbf{Q}, T)|^2 = \prod_{\mathbf{q}\nu} \sqrt{\frac{\omega_{\mathbf{q}\nu}}{\pi}} \exp\left(\frac{-\omega_{\mathbf{q}\nu} Q_{\mathbf{q}\nu}^2}{2n_{\mathbf{q}\nu}(T) + 1}\right) \quad (3)$$

is the squared ground-state wavefunction for non-interacting phonons at $T = 0$ (or the corresponding ensemble average for finite T , $n_{\mathbf{q}\nu}(T) = (\exp(\omega_{\mathbf{q}\nu}/(k_B T)) - 1)^{-1}$ is the Bose-Einstein distribution). Our approximation neglects the kinetic energy of the phonons in the final states and assumes that $k_B T$ is small compared with the electronic energy scale. We use the fact that there is no electron-phonon coupling for the initial state in the undoped t - J model.

In practice, Eq. (2) can be evaluated efficiently by Monte Carlo sampling over the phonon coordinates using $|\phi_0(\mathbf{Q}, T)|^2$ as the weighting function. Each sampled $\rho_{\mathbf{k}}(\mathbf{Q}, \omega)$ requires only the calculation of a purely electronic problem. There is no blow-up of the Hilbert space through the inclusion of dynamic phonons that usually prevents calculations for strong coupling.

To obtain ARPES spectra for La_2CuO_4 we describe the electronic system by the two-dimensional t - J model choosing $t = 0.4$ eV and $J = 0.3t$. $\rho_{\mathbf{k}}(\mathbf{Q}, \omega)$ is calculated using exact diagonalization on a 4×4 cluster with periodic boundary conditions. To check our method we

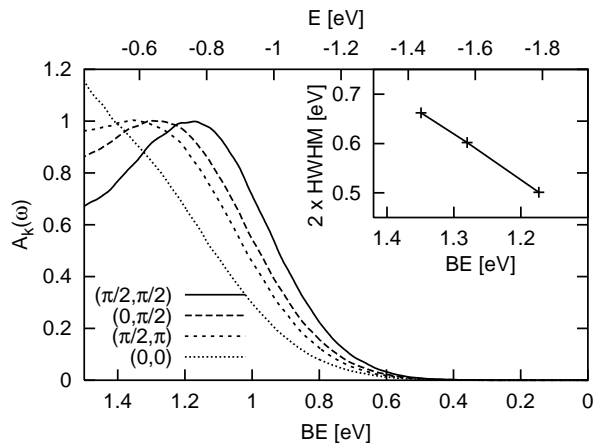


FIG. 3: ARPES spectra for the undoped system at $T = 0$ for different \mathbf{k} normalized to the height of the phonon side band. The lower abscissa shows binding energies (BE) and the upper abscissa the energies of the final states corresponding to the spectral features. The inset shows the dependence of the width of the phonon side band on its binding energy. The width of the $(0, 0)$ spectrum is poorly defined and not shown.

have first assumed a simple Holstein-type of coupling to one dispersionless mode as in Ref. [5] and found good agreements with their results. But our method allows us to include all 21 modes with the \mathbf{q} -dependent coupling given by Eq. (1) [12].

We have calculated $A_{\mathbf{k}}(\omega, T = 0)$ for different values of \mathbf{k} as shown in the main part of Fig. 3. For each spectrum 50000 samples were used. The poles in the sampled spectra were broadened by Gaussians with a FWHM of 33 meV. The spectra show a broad phonon side band which disperses like the quasi-particle in the t - J model without phonons, as was found in Ref. [5]. As shown in Ref. [11] this can be understood easily within our adiabatic approximation. The true quasi-particle peak is almost completely suppressed in weight and dispersion and determines the energy zero on the lower abscissa in Fig. 3. The half-width (HWHM) of the side band is determined on the low binding energy side. We obtain a width of $2 \times \text{HWHM} = 0.5$ eV for $\mathbf{k} = (\pi/2, \pi/2)$, in good agreement with the corresponding experimental result 0.48 eV (cf. bold curves in Fig. 1).

Width and position of the phonon side band as well as the position of the quasi-particle peak are shown in Fig. 4 as a function of the relative coupling strength Λ (substituting $g_{\mathbf{q}\nu} \rightarrow \Lambda g_{\mathbf{q}\nu}$ in Eq. (1)) for $\mathbf{k} = (\pi/2, \pi/2)$ at $T = 0$. For small Λ , the position of the quasi-particle peak [13] starts out at the energy obtained in the t - J model without phonons and approaches for stronger couplings asymptotically the curve given by $-\sum_{\mathbf{q}\nu} \Lambda^2 |g_{\mathbf{q}\nu}|^2 / \omega_{\mathbf{q}\nu} + \text{const.}$ A fully localized hole obtains this energy gain from interaction with phonons (the additional constant depends on the definition of the energy offset). The position of the phonon side band shows

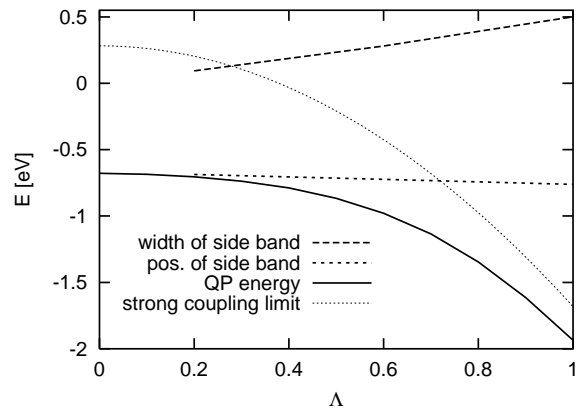


FIG. 4: Width and position of the phonon side band and the position of the quasi-particle peak as a function of the relative coupling strength Λ for $\mathbf{k} = (\pi/2, \pi/2)$.

only a weak linear dependence on Λ . The energy difference to the position of the true quasi-particle peak determines the binding energy. The value of almost 1.2 eV at full coupling is larger than the experimental value of about 0.5 eV (cf. Fig. 1). Since the binding energy depends strongly on doping, a possible explanation for this discrepancy could be that the experimental samples were actually lightly doped. Our shell model calculation could also overestimate the coupling strength. As seen in Fig. 4, the binding energy of the side band has a much stronger dependence on Λ than the width. For $\Lambda = 0.8$, e.g., one would find a width of about 0.4 eV and a binding energy of about 0.6 eV, both quantities being in reasonable agreement with experimental values. As $\lambda \propto \Lambda^2$, this would reduce the dimensionless coupling constant to $\lambda = 0.75$. Such a reduction could be due to a slight underestimate of the screening in the shell model or an overestimate of the coupling to breathing phonons.

The inset in Fig. 3 shows that the width of the phonon side band increases roughly linearly with its binding energy. This trend has also been found experimentally for weakly doped $\text{Ca}_{2-x}\text{Na}_x\text{CuO}_2\text{Cl}_2$ [1]. To understand this, we introduce rescaled phonon coordinates $R_{\mathbf{q}\nu} = \sqrt{\omega_{\mathbf{q}\nu} / (2n_{\mathbf{q}\nu}(T) + 1)} Q_{\mathbf{q}\nu}$. The weighting function in Eq. (3) then becomes invariant under rotations in \mathbf{R} space, and Eq. (2) can be expressed as a sampling over directions for fixed $R = |\mathbf{R}|$ followed by an integration over R . If the \mathbf{R} space has dimension d , the R -integral contains a factor $R^{d-1} e^{-R^2}$, which peaks strongly at $\tilde{R} \equiv \sqrt{(d-1)/2}$. Fig. 5 shows how the contributions to the spectrum evolve with increasing R up to \tilde{R} . Poles in the sampled spectra were broadened by Gaussians with a FWHM of 11 meV. In the figure, the coupling to the $\mathbf{q}=(0,0)$ modes is not included, since it contributes the same broadening for all \mathbf{k} . We focus on peaks to the right, at the lowest binding energies. For $R = 0$, which corresponds to zero electron-phonon cou-

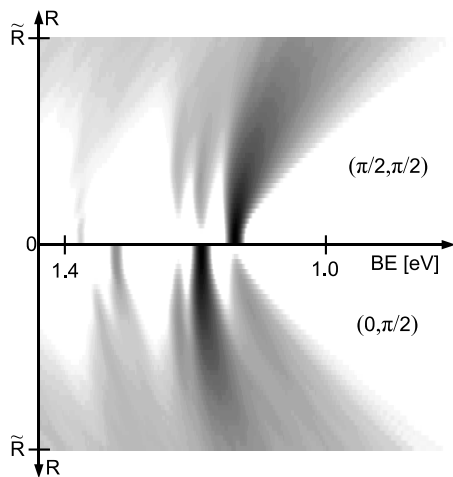


FIG. 5: Contributions to the spectra with $\mathbf{k} = (\pi/2, \pi/2)$ and $\mathbf{k} = (0, \pi/2)$ at $T = 0$ for varying R . Higher spectral weight is represented by darker shading. The abscissa shows binding energies (BE). Coupling to $\mathbf{q} = (0, 0)$ modes is not included.

pling, the spectrum for $\mathbf{k} = (\pi/2, \pi/2)$ has a peak at smaller binding energy than for $\mathbf{k} = (0, \pi/2)$. As R increases and the electron-phonon coupling is switched on, both peaks are broadened. This is due to the repulsion from higher states, which increases with R , but is different for different directions of \mathbf{R} . For the peak with the lowest binding energy this broadening is largest, since all the other states repel the corresponding state in the same direction. Fig. 3 shows, however, the opposite trend for the width of the phonon side band in the final spectra, due to the following opposing effect which dominates. For $R \neq 0$ spectral weight also appears at energies with no peaks in the $R = 0$ spectra. For $R \neq 0$, the system is distorted and the electronic momentum \mathbf{k} is not conserved. For instance, in case of $\mathbf{k} = (0, \pi/2)$, a peak of increasing width and weight appears at the energy of the main peak in the $\mathbf{k} = (\pi/2, \pi/2)$ spectrum. At $R = \tilde{R}$, these side bands have more or less merged with the main peak and effectively add to its width. For $\mathbf{k} = (\pi/2, \pi/2)$ there is no such extra contribution for lower binding energies whereas for $\mathbf{k} = (0, \pi/2)$ the width is increased by one side band. There are more and more side bands on the low binding energy side of the main peak as the binding energy of the main peak increases, which increases the width of the resulting broad peak on the low binding energy side.

Finally, we have studied the temperature dependence of the width of the phonon side band. It is relatively weak. For $\mathbf{k} = (\pi/2, \pi/2)$ it increases from 500 meV at $T = 0$ to 565 meV at $T = 200$ K and 750 meV at $T = 400$ K. The main contribution to the T dependence is due to the modes with an energy of about 20 meV.

To summarize, we have shown that the polaronic fea-

tures in ARPES spectra of La_2CuO_4 and other undoped cuprates can be attributed to strong coupling between the photo hole and phonons. This electron-phonon coupling is due to the modulation of the electrostatic potential and the singlet energy. We have introduced an efficient method for obtaining ARPES spectra in undoped systems and shown that with the derived coupling there is good agreement with experimental results. The dependence of the width of the broad phonon side band on binding energy and temperature has also been discussed. Our results show the importance of electron-phonon coupling for the physics of undoped cuprates.

We thank T. P. Devereaux and P. Prelovšek for useful discussions.

-
- [1] K. M. Shen, F. Ronning, D. H. Lu, W. S. Lee, N. J. C. Ingle, W. Meevasana, F. Baumberger, A. Damascelli, N. P. Armitage, L. L. Miller, Y. Kohsaka, M. Azuma, M. Takano, H. Takagi, and Z.-X. Shen, *Phys. Rev. Lett.* **93**, 267002 (2004).
 - [2] S. L. Chaplot, W. Reichardt, L. Pintschovius, and N. Pyka, *Phys. Rev. B* **52**, 7230 (1995).
 - [3] O. Rösch and O. Gunnarsson, *Phys. Rev. Lett.* **92**, 146403 (2004).
 - [4] L. Pintschovius and W. Reichardt, in *Neutron Scattering in Layered Copper-Oxide Superconductors*, edited by A. Furrer, Physics and Chemistry of Materials with Low Dimensional Structures, Vol. 20 (Kluwer Academic, Dordrecht, 1998), p. 165.
 - [5] A. S. Mishchenko and N. Nagaosa, *Phys. Rev. Lett.* **93**, 036402 (2004).
 - [6] The finite number of mesh points leads to an underestimate of λ by about 3% for a $(30)^3$ mesh.
 - [7] X. J. Zhou, J. Shi, T. Yoshida, T. Cuk, W. L. Yang, V. Brouet, J. Nakamura, N. Mannella, S. Komiya, Y. Ando, F. Zhou, W. X. Ti, J. W. Xiong, Z. X. Zhao, T. Sasagawa, T. Kakeshita, H. Eisaki, S. Uchida, A. Fujimori, Z. Zhang, E. W. Plummer, R. B. Laughlin, Z. Hussain, and Z.-X. Shen, *cond-mat/0405130*.
 - [8] A. Bianconi, N. L. Saini, A. Lanzara, M. Missori, T. Rossetti, H. Oyanagi, H. Yamaguchi, K. Oka, and T. Ito, *Phys. Rev. Lett.* **76**, 3412 (1996).
 - [9] E. S. Bozin, G. H. Kwei, H. Takagi, and S. J. L. Billinge, *Phys. Rev. Lett.* **84**, 5856 (2000).
 - [10] L. Tassini, F. Venturini, Q.-M. Zhang, R. Hackl, N. Kikugawa, and T. Fujita, *cond-mat/0406169*.
 - [11] O. Rösch and O. Gunnarsson, *Eur. Phys. J. B* **43**, 11 (2005); K. Schönhammer and O. Gunnarsson, *Phys. Rev. B* **30**, 3141 (1984).
 - [12] The q_z dependence is unimportant as the electronic model is purely two-dimensional. For given q_x, q_y, ν we therefore use a single mode with effective coupling $g_{\text{eff}} = \sqrt{\sum_{q_z} |g_{q_z}|^2}$ and frequency $\omega_{\text{eff}} = g_{\text{eff}}^2 / \sum_{q_z} (|g_{q_z}|^2 / \omega_{q_z})$.
 - [13] The position of the true quasi-particle peak is obtained from a simulated annealing search over the adiabatic energy surface.